TASK QUARTERLY 5 No 4 (2001), 595–602

NUMERICAL INVESTIGATION OF FLOW IN MIXED-FLOW PUMP WITH VOLUTE

MILAN SEDLAR

SIGMA Research and Development Institute,
Jana Sigmunda 79, 78350 Lutin, Czech Republic
sigmavvu@mbox.vol.cz

(Received 12 July 2001)

Abstract: This work deals with modelling of flow in a complete mixed-flow pump with volute, including the tip leakage flows, using both the quasi-steady and true transient models of rotor/stator interaction. The CFX-TASCflow CFD package from AEA Technology is applied to calculate flows for a wide range of flow rates from about 0.2 to $1.4\,Q_{\mathrm{opt}}$. Fairly detailed flow structures have been predicted based on the flow rates, especially the impeller inlet recirculation and separations on the suction side of the blades for the suboptimal rates of flow, as well as strong secondary flows and separations in the volute for off-design conditions. The rotor/stator interaction influence on flow phenomena both in the impeller and volute have been investigated with very interesting results, providing a good insight into the dynamics of flow close to the volute tongue. Based on the computational results, pump performance curves (Q-H, Q-η_{h} and Q-P, η_{h} being the hydraulic efficiency) have been obtained. The data from this numerical investigation have been used to improve the inlet part of the impeller blades, especially close to the tip. The geometry modifications have resulted in reducing cavitation in the impeller as well as the noise at suboptimal rates of flow.

Keywords: CFD, separated flow, cavitation, unsteady phenomena, mixed-flow pump, volute

1. Introduction

In recent years, there has been some great improvement in analysing 3D turbulent flows through axial-flow or mixed-flow machinery. Not long ago calculations were devoted largely to the single component flow analysis, rarely including tip leakage flow. Here, different grid topologies were used to simulate flows in the tip clearance gap. Some papers also took into account the interaction of rotating and stationary parts, however simple quasi-steady interaction models were more widely used than the true transient ones. Nowadays, new developments in CFD, including robust rotor/stator interaction algorithms, new turbulence models or advanced grid generation techniques, enable us to model flow fields effectively in such a complex geometry as the complete axial-flow or mixed-flow machine.

Mixed-flow pumps BQO series are produced mainly for the irrigation and drainage purposes. Large fluctuations of the water level require a large operation range and so pumps operate often at off-design conditions. At these regimes backflow can be found both in the impeller and volute, together with increased noise and vibration level. When tested

on the test rig, BQO pumps demonstrated increased noise and vibrations with their peak at the flow rate about $0.6-0.75\,Q_{opt}$, according to the pump size. The aim of this work was to predict numerically flow in a model BQO pump, including the tip leakage flows and cavitation phenomena, applying both the quasi-steady and true transient models of rotor/stator interaction.

2. Calculation details

The pump geometry was processed with CFX-Bladegen preprocessor from AEA Technology, following with ICEM CFD grid generation means. The CFX-TASCflow CFD package has been applied to solve the three-dimensional Reynolds-averaged Navier-Stokes equations using the finite element based finite volume method in strong conservation form [1]. The second-order Linear Profile Skewed Upstream Differencing Scheme with Physical Advection Correction has been applied to obtain high accuracy. The code provides multi-block boundary fitted grids with local grid refinement and general grid interface. Advanced concept of grid embedding and connecting together dissimilar grid regions allows one to form the grid close to the tip clearance gap. To model turbulent quantities, RNG k-ε turbulence model has been applied. To analyse the interaction of stationary and rotating components, the Frozen Rotor Method as well as True Transient Simulation capabilities have been used [2].

The geometry of the mixed-flow pump consists of the impeller with four blades, including tip gaps, and a volute (Figure 1), with pieces of circular pipes at the impeller inlet and the volute outlet, so that both impeller inlet recirculations and separations in the volute could be modelled. The computational grid includes 20 structured blocks with about 540 000 nodes. Boundary conditions are specified in the relative frame of reference, and consequently all solid walls of the impeller and the volute are stationary except for the impeller casing, which rotates at the blade speed in the opposite direction of the impeller. On all the walls, wall functions have been applied. At the inlet, velocity, turbulent kinetic energy and its dissipation rate have been prescribed according to flow rates and estimated turbulent intensity and eddy length scale. At the outlet, the average static pressure has been set. At the axis of revolution in front of the impeller, the symmetry condition has been applied. When using the Frozen Rotor Method, six different positions of the impeller and volute have been used [3]. When using the True Transient Simulation, 180 time steps represent one impeller revolution. In both cases the frame interface is situated between the impeller and volute; no frame interface has been applied between the blade tip and the impeller casing.

Cavitation properties have been investigated using the Constant Enthalpy Vaporization model, implemented in CFX-TASCflow. This model is suitable especially for prediction of attached vapour cavities, however, it is less suitable for predicting tip clearance and tip vortex cavitation phenomena [4, 5].

3. Results and discussion

Flow rates range from about 0.2 to $1.4\,Q_{opt}$. Eleven flow rates have been applied to cover this interval. Based on the computational results, pump performance curves (Q-H, Q-η_h and Q-P, η_h being the hydraulic efficiency) have been obtained (Figure 2, red lines). The optimal flow rate predicted is $Q_{opt} = 260$ l/s.

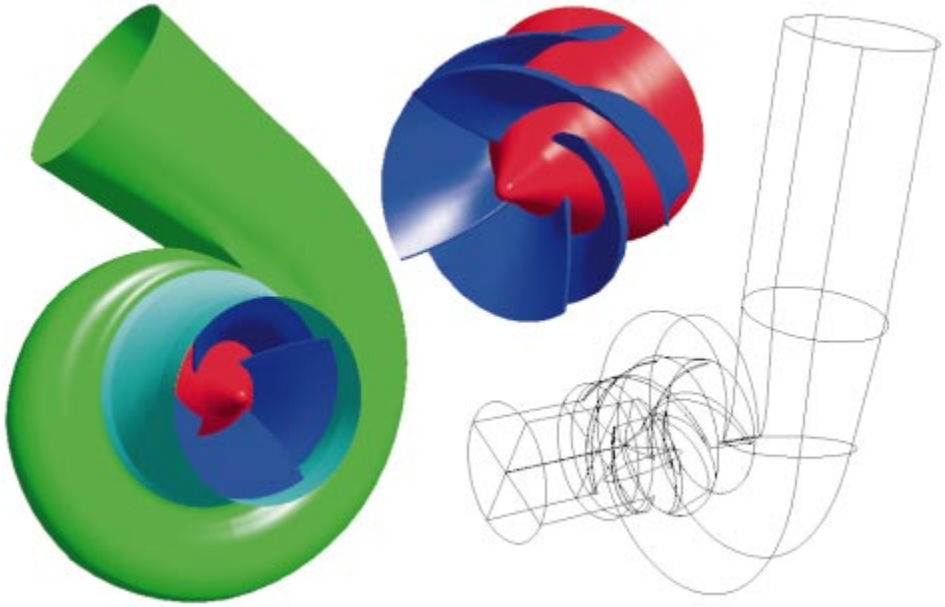

Figure 1. Geometry of pump and grid structure

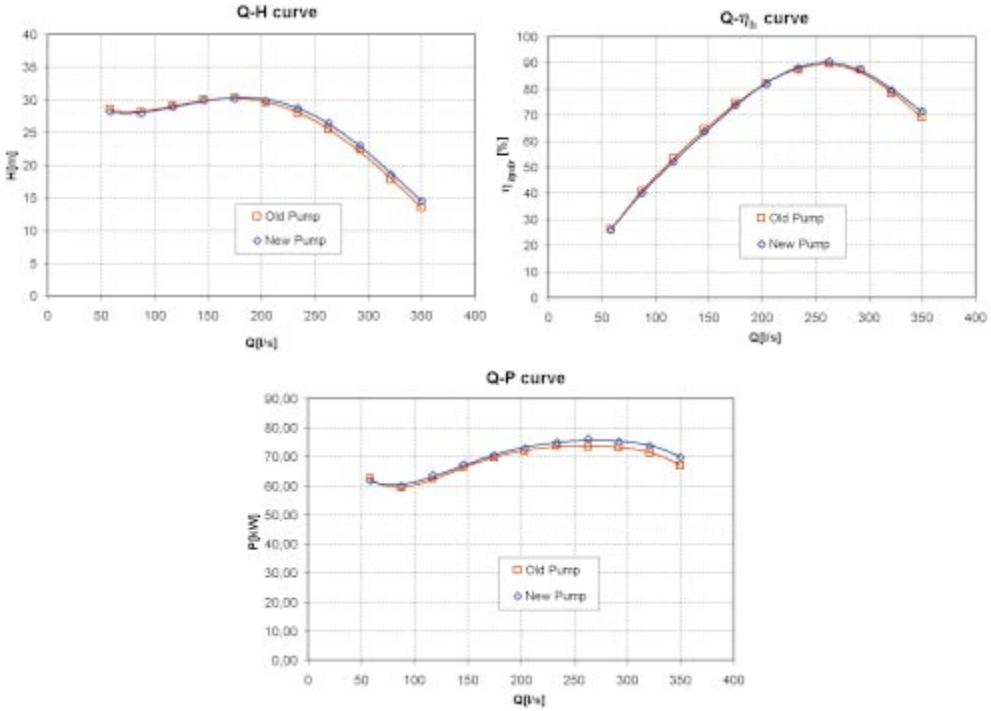

Figure 2. Pump performance curves

Detailed flow structures have been predicted based on the flow rates, especially the impeller inlet recirculation and separations on the suction side of the blades for the suboptimal rates of flow, as well as strong secondary flows and separations in the volute for

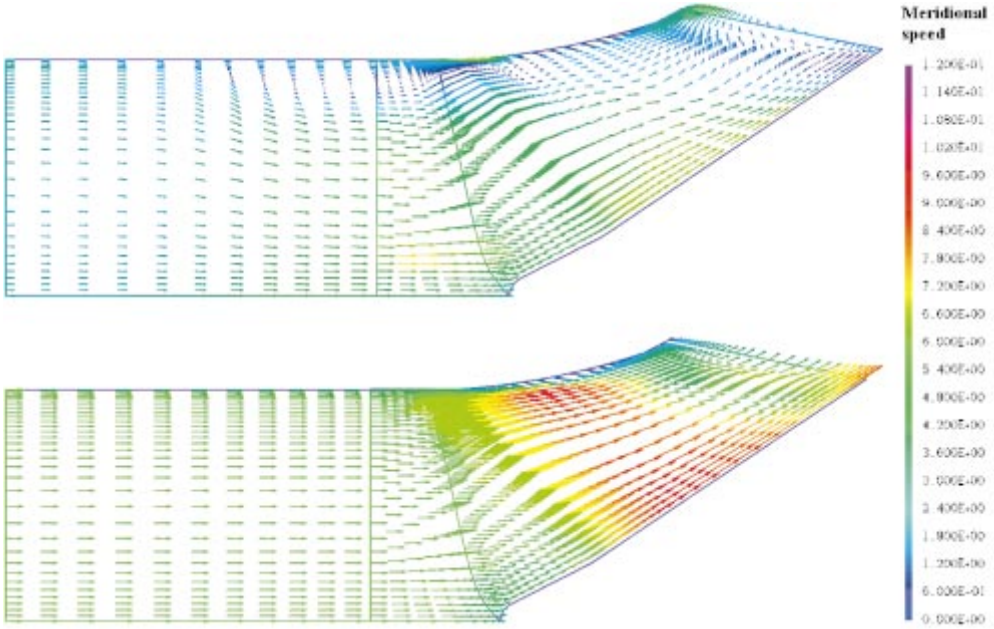

Figure 3. Meridional flow at midpitch of an impeller passage for the flow rates of $0.56\,Q_{\text{opt}}$ and $1.12\,Q_{\text{opt}}$

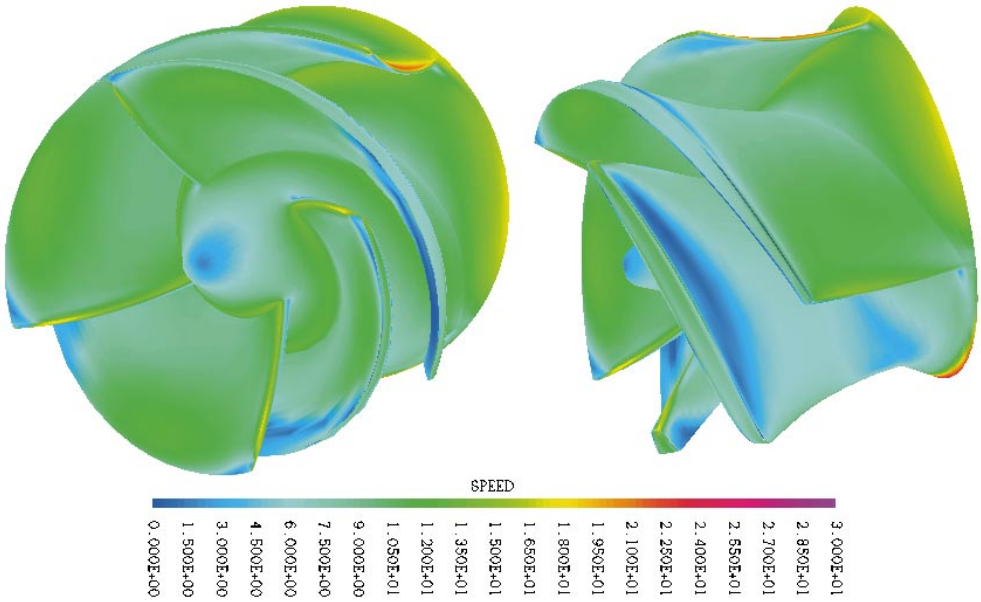

Figure 4. Velocity distribution close to the impeller surface for the flow rate of $0.45\,Q_{\text{opt}}$

off-design conditions. Meridional flow field in the impeller shows a backflow for the whole range of flow. For the flow rates higher than $0.7\,Q_{\text{opt}}$ the backflow is attached to the shroud side in a very narrow layer and does not reach the impeller leading edges. For the flow rates lower than $0.7\,Q_{\text{opt}}$ the backflow propagates downstream the impeller leading edges

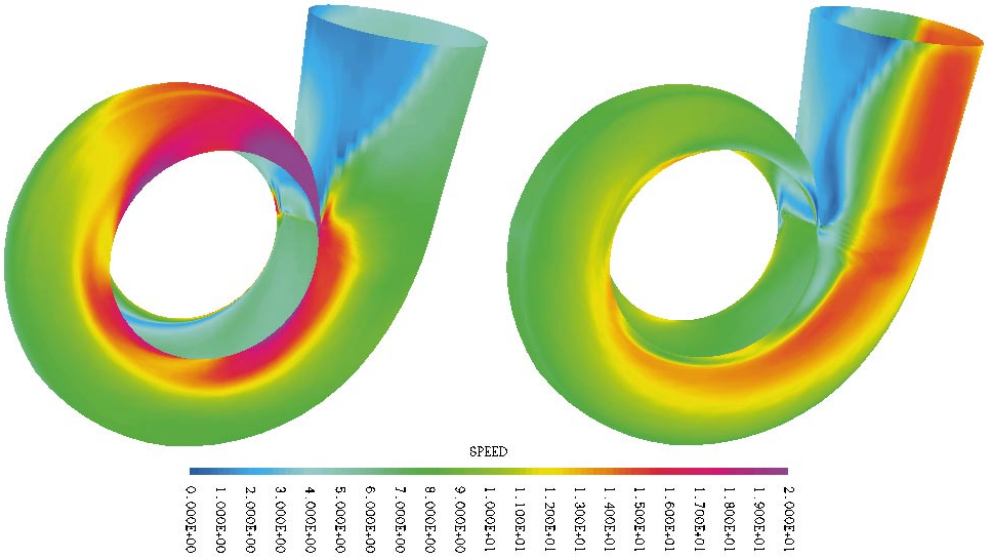

Figure 5. Velocity distribution close to the volute surface for the flow rates of $0.45\,Q_{\mathrm{opt}}$ and $1.35\,Q_{\mathrm{opt}}$

and the impeller inlet recirculation width grows fast with decreasing flow rate. Figure 3 shows the meridional flow at midpitch of an impeller passage for the flow rates of $0.56\,Q_{\mathrm{opt}}$ (top) and $1.12\,Q_{\mathrm{opt}}$ (bottom). At the flow rate of $0.67\,Q_{\mathrm{opt}}$ small separation regions appear at the blade tip both on the suction and pressure sides of the leading edge, as well as on the suction side at about 60% and on the pressure side at about 40% of the chord length. Backflow increases with decreasing flow rate and propagates from the blade tip towards the hub side. At the flow rate of $0.225\,Q_{\mathrm{opt}}$ separation on the pressure side reaches the impeller hub. Very important is the fact that the separated flow is highly unsymmetrical for very small flow rates (see Figure 4, showing velocity distribution close to the impeller surface for the flow rate of $0.45\,Q_{\mathrm{opt}}$).

There is a very complex three-dimensional flow in the volute. For the whole range of flow secondary flows can be observed, the intensity of which has its minimum for the flow rates close to optimum. For the flow rates outside the interval $(0.67\,Q_{\mathrm{opt}},\ Q_{\mathrm{opt}})$ backflow appears in the volute (see Figure 5, showing velocity distribution close to the volute surface for the flow rates of $0.45\,Q_{\mathrm{opt}}$ and $1.35\,Q_{\mathrm{opt}}$). At suboptimal rates of flow there is a flow separation on the impeller side of the volute tongue but also practically no flow in the direction of the discharge branch axis can be found on the outer side of the tongue and adjacent side of the discharge branch. For superoptimal flow rates a large separation can be seen covering the outer part of the tongue and adjacent side of the discharge branch. At very high rates of flow we can also detect a small separation region on the impeller side of the tongue. For the flow rates below $0.9\,Q_{\mathrm{opt}}$ a separation appears also on the sidewalls of the volute. It is important to note that the backflow in the volute changes significantly in time according to the position of the impeller blade and the volute tongue.

The rotor/stator interaction influence on flow phenomena both in the impeller and volute has been investigated with very interesting results, providing a good insight into the dynamics of flow. It has been found from the frozen rotor and true transient simulations that the separations inside the pump are highly instationary phenomena for all flow regimes,

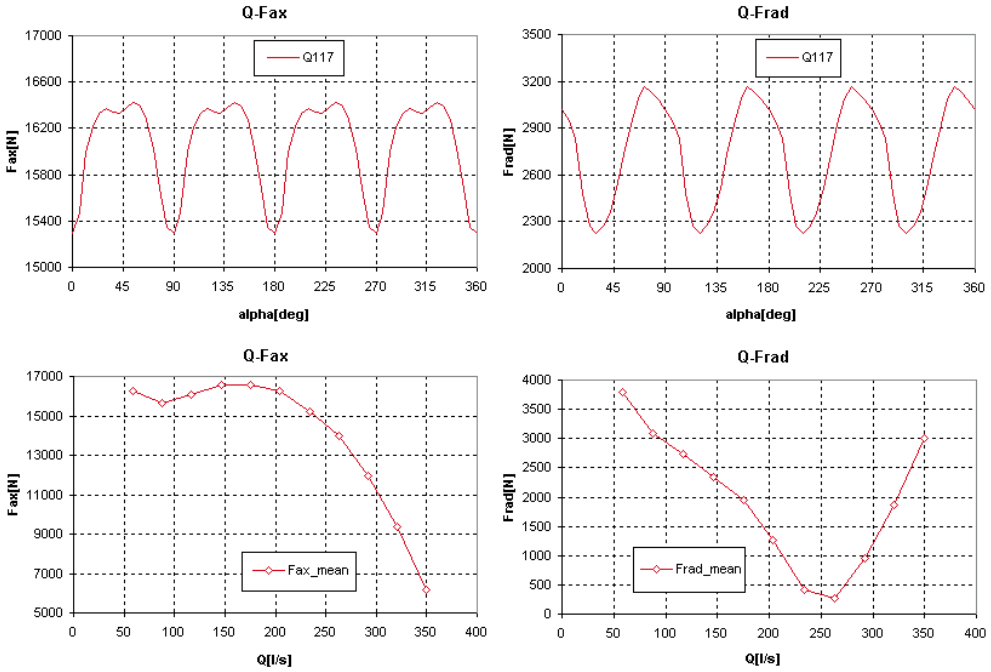

Figure 6. Axial and radial thrust on the impeller for the flow rate of $0.45\,Q_{\mathrm{opt}}$ during one revolution and mean values of axial and radial thrust for different flow rates

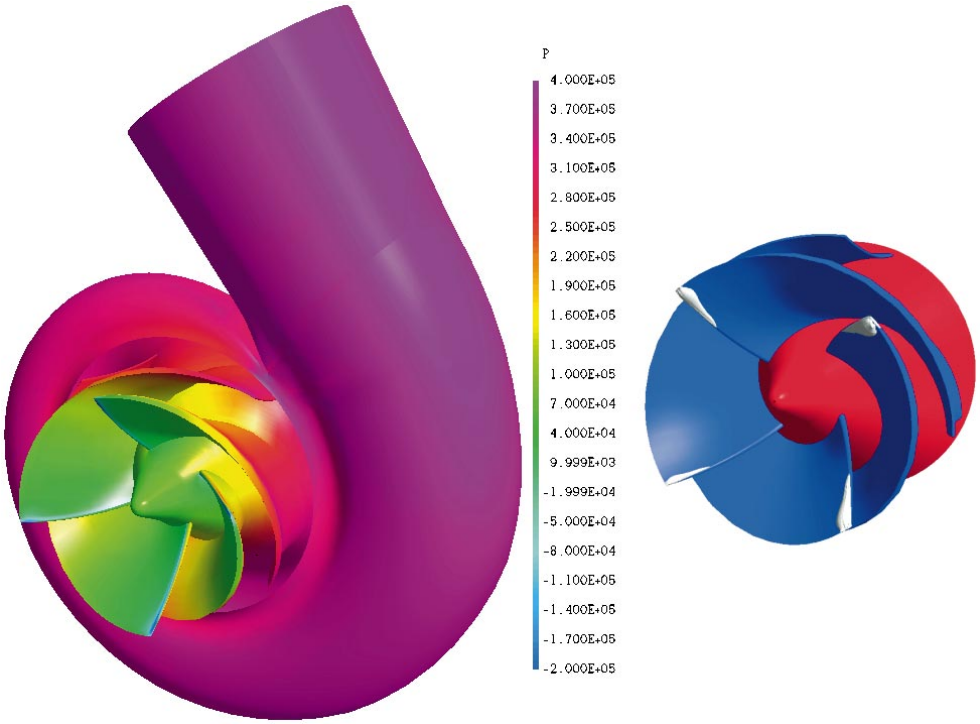

Figure 7. Pressure distribution on pump solid walls for noncavitating flow calculation and cavitation regions in the impeller calculated for the flow rate of $0.67\,Q_{\mathrm{opt}}$ and the suction head of 2.5 m

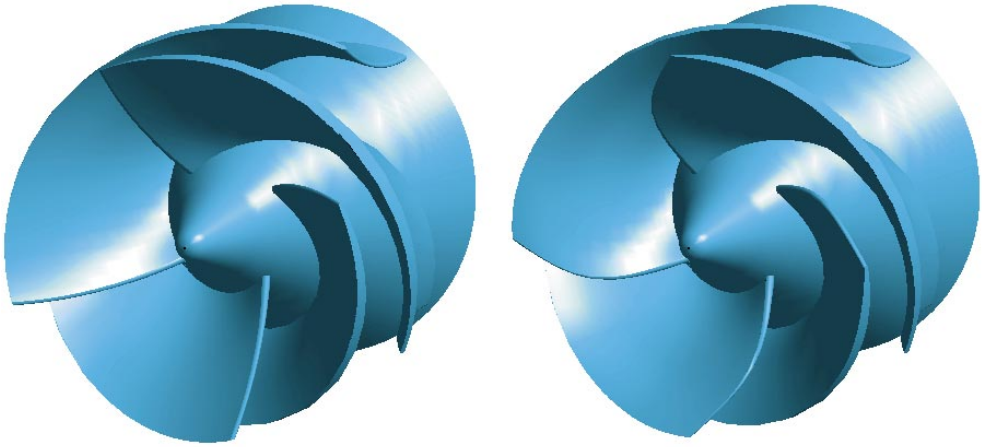

Figure 8. Comparison of the old and new geometries of the impeller

including flow rates close to the optimal one. For example at the flow rate of $1.12\,Q_{\text{opt}}$ separation in the volute changes from zero length to the separation starting just behind the cut-water and nearly reaching the end of the discharge branch. Very important is the fact that the true transient simulation made it also possible to study in detail axial and radial forces acting on impeller, including the fluctuating part of forces. Figure 6 shows mean components of axial and radial forces acting on the impeller, as a function of flow rate (bottom), and the variation of the axial and radial forces for 45% of the optimal flow rate (top), based on the blade and volute tongue position. Position zero is when the trailing edge of the blade at the tip is aligned with cut-water. The maximum radial load is obtained when the pressure side back part is aligned with the cut-water (in the position when the fluid flows in the absolute frame of reference just from the trailing edge towards the volute tongue and meets the cut-water), which is in good agreement with results presented in [6]. The minimum radial load is at the 30° position. The axial load has not such a sharp maximum. On the other hand there is a sharp minimum at the 0° position and a local minimum at the 42° position. As it can be seen from Figure 6, the variation of the axial thrust is lower than 10% of the mean value while for the radial force this rate represents nearly 40%.

When calculating noncavitating flows in the pump for the supposed suction head of 2.5 m, regions with the static pressure below the vapour pressure have been detected close to the leading edges of the impeller blades (Figure 7 left). Following cavitation modelling has shown that the largest vapour cavities appear at the flow rate of $0.67\,Q_{\text{opt}}$ on the suction side of blades, at the blade tip behind the leading edge (Figure 7 right). With the decreasing flow rate these cavities decrease and move towards the hub side. With the increasing flow rate the cavitation decreases as well and the cavities move to the pressure side, just behind the leading edge at the blade tip. It corresponds well to the noise level measurements on the test rig.

4. Conclusions

The flow in a model BQO pump, including the tip leakage flows and cavitation phenomena, has been investigated numerically. Both the quasi-steady and true transient

models of rotor/stator interaction have been applied. Flow rates range from about 0.2 to 1.4 Q_{opt}. Detailed flow structures have been predicted basing on the flow rates, especially the impeller inlet recirculation and separations on the suction and pressure sides of the blades for the suboptimal rates of flow, as well as strong secondary flows and separations in the volute for off-design conditions. The rotor/stator interaction influence on flow phenomena both in the impeller and volute has been investigated with very interesting results, providing a good insight into the dynamics of flow close to the volute tongue.

The data from this numerical investigation have been used to improve the inlet part of the impeller blades, especially close to the tip (see Figure 8). The geometry modifications result in reducing calculated vapour cavities on the suction side of the blades behind the leading edge. On the test rig this new hydraulic design has demonstrated significant fall in noise at suboptimal rates of flow. The efficiency of the new machine has increased at the best efficiency point by 1% (see Figure 2).

Acknowledgements

This work has been supported by the Grant Agency of CAS S2076003 "Suppression of Onset and Effects of Cavitation in Hydrodynamic Machines".

References

[1] TASCflow CFD Software – User Documentation, 1999, AEA Technology, Waterloo, Ontario

[2] Galpin P F, Bronberg R B and Hutchinson B R 1995 *Three-Dimensional Navier Stokes Predictions of Steady State Rotor/Stator Interaction with Pitch Change* Proc. Third Conference of the CFD Society of Canada

[3] Sedlar M, Vlach M and Soukal J 1999 *Numerical and Experimental Investigation of Flow in Axial-Flow Hydraulic Machinery* Proc. 3^{rd} European Conf. On Turbomachinery, London, pp. 1007 – 1016

[4] Laborde R, Chantrel P and Mory M 1997 *Journal of Fluids Engineering* **119** 680

[5] Sedlar M, Marsik F and Safarik P 2000 *Modelling of Cavitated Flows in Hydraulic Machinery Using Viscous Flow Computation and Bubble Dynamics Model* Proc. Fluid Dynamics Prague, pp. 107 – 110

[6] Goulas A and Truscott G F 1986 *Dynamic Hydraulic Loading on a Centrifugal Pump Impeller* Proc. Radial Loads and Axial Thrust on Centrifugal Pumps, London, pp. 53 – 64